THE JOURNAL OF PHYSICAL CHEMISTRY A

Article

pubs.acs.org/JPCA

Coupled Cluster Evaluation of the Stability of Atmospheric Acid–Base Clusters with up to 10 Molecules

Nanna Myllys,[†] Jonas Elm,[*,†] Roope Halonen,[†] Theo Kurtén,[‡] and Hanna Vehkamäki[†]

[†]University of Helsinki, Department of Physics, FIN-00014 Helsinki, Finland

[‡]University of Helsinki, Department of Chemistry, FIN-00014 Helsinki, Finland

Supporting Information

ABSTRACT: We investigate the utilization of the domain local pair natural orbital coupled cluster (DLPNO-CCSD(T)) method for calculating binding energies of atmospherical molecular clusters. Applied to small complexes of atmospherical relevance we find that the DLPNO method significantly reduces the scatter in the binding energy, which is commonly present in DFT calculations. For medium sized clusters consisting of sulfuric acid and bases the DLPNO method yields a systematic underestimation of the binding energy compared to canonical coupled cluster results. The errors in the DFT binding energies appear to be more random, while the systematic nature of the DLPNO results allows the establishment of a scaling factor, to better mimic the canonical coupled cluster calculations. Based on the trends identified for the small and medium sized systems, we further extend the application of the DLPNO method to large acid - base clusters consisting of up to 10 molecules, which have previously been out of reach with accurate coupled cluster methods. Using the Atmospheric Cluster Dynamics Code (ACDC) we compare the sulfuric acid dimer formation based on the new DLPNO binding energies with previously published RI-CC2/aug-cc-pV(T+d)Z results. We also compare the simulated sulfuric acid dimer concentration as a function of the base concentration with measurement data from the CLOUD chamber and flow tube experiments. The DLPNO method, even after scaling, underpredicts the dimer concentration significantly. Reasons for this are discussed.

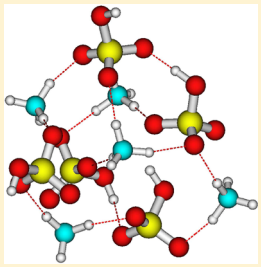

1. INTRODUCTION

Intermolecular hydrogen-bonding interactions are responsible for the formation of molecular clusters in the atmosphere.[1] Through a clustering mechanism atmospheric vapors can be converted into aerosol particles.[2] Atmospheric aerosols are important for Earth's radiation balance, counteracting the warming effect of greenhouse gases, by scattering radiation back into space. The formation of new particles is not yet understood but is believed to often involve sulfuric acid coupled to a stabilizing component, such as ammonia,[3−8] amines,[9−21] or nonbasic oxidized organic compounds.[22−44] Computational methods are an important tool to explore the initial steps in new particle formation, as small clusters are difficult to detect experimentally. Furthermore, the composition of neutral clusters cannot be measured directly, as charging necessarily carries the risk of changing the cluster composition. Calculated Gibbs free energies can be used to establish cluster stabilities and, together with estimates of collision rates and the detailed balance assumption, evaluate the cluster population dynamics using for example the Atmospheric Cluster Dynamics Code (ACDC).[45−47] Highly accurate ab initio calculations on atmospheric molecular clusters are valuable but limited to small clusters due to the steep scaling of computational cost with respect to system size. Shields and coworkers have published four papers on MP2/CBS and CCSD(T)/CBS calculations for small systems to illuminate the importance of hydration of various atmospheric species: hydration of sulfuric acid and the sulfuric acid dimer by Temelso et al.,[48,49] the atmospheric implication of the hydration of the bisulfate ion by Husar et al.,[50] and the hydration of the sulfuric acid−methylamine complex by Bustos et al.[51]

Obtaining information about larger clusters is essential to bridge the gap between theory and experiments. Density functional theory is a popular choice for estimating the geometries and thermochemistry for the formation of larger atmospheric molecular clusters. Benchmarks utilizing either accurate computational Gibbs free energies or carefully conducted experiments are sparse but extremely valuable in the assessment of the performance of different DFT functionals.[52−54] Using a large test set of atmospheric molecular clusters, we have recently evaluated DFT binding energies against coupled cluster results[55] and tested how the thermal contribution to the Gibbs free energy depends on the choice of functional.[56] The DFT binding energies were found to be the largest source of errors when evaluating the free energies of strongly hydrogen bonded atmospheric molecular clusters. This work further extends our analysis to assess the feasibility of higher level ab initio methods to obtain the binding energies. Different approximations can be invoked to apply accurate ab initio methods beyond medium-sized systems. Using density fitting (DF)/resolution of identity (RI) methods the computational scaling can be significantly reduced with respect to basis set size.[57,58] The emergence of explicitly correlated methods significantly improves the slow convergence of the electron

Received: October 6, 2015
Revised: January 15, 2016
Published: January 15, 2016

DOI: 10.1021/acs.jpca.5b09762
J. Phys. Chem. A 2016, 120, 621−630

correlation energy with respect to the basis set size.[59−61] Another common approach is to utilize localized orbitals, which will allow calculations on significantly larger systems. Recently, Riplinger and Neese developed a domain local pair natural orbital coupled cluster method (DLPNO-CCSD(T)).[62,63] This is the first black-box-localized coupled cluster method that allowed the calculation of the single-point energy of an entire Crambin protein (644 atoms). The DLPNO-CCSD(T) method differs slightly from the corresponding canonical methods by employing the T_0 approximation for evaluating the triples. The T_0 approximation neglects all off-diagonal Fock Matrix elements and thereby yields a significant computational speed-up. Employing the T_0 approximation should recover ∼97% of the full local triple correction.[63] We investigate the applicability of the DLPNO-CCSD(T) method in the context of atmospheric new particle formation. We initially benchmark the DLPNO-CCSD(T) method against explicitly correlated canonical coupled cluster methods for small complexes of atmospheric relevance. The analysis is extended to medium-sized clusters consisting of sulfuric acid and ammonia/dimethylamine. On the basis of these results, we further extend the analysis to larger clusters and apply the DLPNO-CCSD(T) method on clusters consisting of up to five sulfuric acid and up to five ammonia/dimethylamine molecules, which have previously been out of reach with accurate coupled cluster methods.

2. COMPUTATIONAL DETAILS

All density functional theory geometry optimizations and frequency calculations have been performed with Gaussian 09.[64] For applying empirical dispersion, Gaussian 09 rev. D was used.[65] The Grimme's D3 version was utilized in all cases.[66] Explicitly correlated coupled cluster calculations have been run using Molpro 2012.[67] Domain-based local pair natural orbital coupled cluster calculations have been performed with ORCA[68] with a def2-QZVPP basis set. Henceforth we will refer to the CCSD(T)-F12a/VDZ-F12 and DLPNO-CCSD(T)/def2-QZVPP levels of theory simply as F12 and DLPNO, respectively. The cluster binding energy and cluster binding Gibbs free energy are calculated as follows

$$\Delta E_{\text{binding}} = E_{\text{cluster}} - \sum_i E_{\text{monomer},i}$$

$$\Delta G_{\text{binding}} = G_{\text{cluster}} - \sum_i G_{\text{monomer},i}$$

From the cluster binding energies the thermal contribution to the Gibbs free binding energy can be calculated

$$\Delta G_{\text{therm}} = \Delta G_{\text{binding}} - \Delta E_{\text{binding}}$$

Unless otherwise noted all thermochemical parameters have been calculated using rigid rotor−harmonic oscillator approximations at 298 K and 1 atm.

3. RESULTS AND DISCUSSION

3.1. Gibbs Free Energies of Small Complexes. To test the variation in the thermal contribution to the Gibbs free energy using different DFT functionals and the accuracy of the DFT and DLPNO binding energies, we initially investigate the following six complex formation reactions

$$(H_2SO_4)(H_2O) + H_2O \leftrightharpoons (H_2SO_4)(H_2O)_2 \quad (2)$$

$$H_2SO_4 + NH_3 \leftrightharpoons (H_2SO_4)(NH_3) \quad (3)$$

$$H_2SO_4 + (CH_3)_2NH \leftrightharpoons (H_2SO_4)((CH_3)_2NH \quad (4)$$

$$H_2SO_4 + HCOOH \leftrightharpoons (H_2SO_4)(HCOOH) \quad (5)$$

$$H_2SO_4 + H_2SO_4 \leftrightharpoons (H_2SO_4)_2 \quad (6)$$

These reactions represent some of the key interactions in atmospheric aerosols, that is, sulfuric acid hydration (reactions 1 and 2), interaction of sulfuric acid with inorganic bases (reaction 3), organic bases (reaction 4), organic acids (reaction 5), and inorganic acids (reaction 6). To obtain the geometries, we tested 11 different DFT functionals with the 6-311++G(3df,3pd) basis set as well as MP2 with the aug-cc-pv(D+d)z and aug-cc-pv(T+d)z basis sets. As a benchmark the binding energy is evaluated at the DFT/MP2 geometries using a high-level explicitly correlated F12 method. All individual binding energies for each reaction can be seen in the Supporting Information. There is a large scatter in the calculated DFT binding energies depending on which functional is utilized, with variations up to 4.0 kcal/mol between PW91 and CAM-B3LYP-D for the formation of the $(H_2SO_4)_2$ complex (see Table S1). We have excluded B3LYP from the analysis due to its known deficiency in calculating binding energies; however, there is little variation between the different functionals in the thermal contribution to the Gibbs free energy. The largest thermal variation is between M11 and B3LYP-D for the $(H_2SO_4)(H_2O)_2$ complex with a difference of 1.1 kcal/mol (see Table S2). This further confirms that the binding energy is the largest source of errors in modeling atmospheric molecular clusters and that the thermal contribution is well reproduced by all functionals. Using coupled cluster single-point energy calculations on top of the DFT/MP2 geometries to obtain the binding energies significantly reduces the scatter with the largest variation being reduced to 0.6 kcal/mol (see Table S3). Table 1 presents the mean absolute error (MAE), mean signed error (MSE), and maximum error (ME) in the DFT/MP2 binding energies compared with F12 results for reactions 1−6.

Table 1. Mean Absolute Error (MAE), Mean Signed Error (MSE), and Maximum Error (ME) in the DFT/MP2 Binding Energy Compared with CCSD(T)-F12a/VDZ-F12[a]

method	ΔE_{MAE}	ΔE_{MSE}	ΔE_{ME}
PW91	1.3	−0.8	2.5
M062X	1.1	−1.0	1.3
ωB97X-D	0.5	−0.5	0.9
B3LYP	1.4	1.4	3.2
PBE0	0.8	−0.2	1.5
CAM-B3LYP	0.9	−0.6	1.4
M11	1.1	−1.1	2.5
M06-2X-D	1.2	−1.1	1.4
B3LYP-D	1.3	−1.3	1.7
PBE0-D	1.9	−1.9	2.5
CAM-B3LYP-D	2.5	−2.5	3.3
MP2/av(D+d)z	0.8	−0.6	2.6
MP2/av(T+d)z	0.9	−0.9	1.8

[a]For all DFT functionals the 6-311++G(3df,3pd) basis set was used. Values are in kcal/mol.

DOI: 10.1021/acs.jpca.5b09762
J. Phys. Chem. A 2016, 120, 621−630

Several of the functionals have a MAE in the binding energy below 1 kcal/mol compared with F12 results. Including empirical dispersion significantly improves the MAE for B3LYP but increases the error for PBE0 and CAM-B3LYP. For M06-2X the results are unaffected by the dispersion correction. The ωB97X-D functional yields binding energies in best agreement with coupled cluster results with a maximum deviation of 0.9 kcal/mol for the formation of the (H_2SO_4)-$((CH_3)_2NH)$ complex. To test the performance of the DLPNO method, we look closer at reaction 6, which posed the largest variations in the binding energy for the DFT/MP2 methods. In Table 2 the binding energies of reaction 6 are seen calculated using DFT with a 6-311++G(3df,3pd) basis set, compared with DLPNO and F12 calculations. The highest and lowest values are marked in bold for each level of theory, excluding B3LYP due to its known deficiency in calculating binding energies. The scatter is reduced from 4.0 to 0.6 kcal/mol when using DLPNO compared with DFT. The scatter in the F12 calculation is seen to be slightly lower than DLPNO with a value of 0.4 kcal/mol.

Table 2. Calculated Binding Energies (ΔE) for the Formation of the $(H_2SO_4)_2$ Complex in Reaction 6 Using DFT/6-311++G(3df,3pd), DLPNO-CCSD(T)/def2-QZVPP, and CCSD(T)-F12a/VDZ-F12[a]

	ΔE_{DFT}	ΔE_{DLPNO}	ΔE_{CC-F12}
PW91	**−17.2**	−17.0	**−17.8**
M062X	−19.1	−17.4	−17.9
ωB97X-D	−18.4	**−17.5**	−17.9
B3LYP	−15.9	−17.2	−17.9
PBE0	−17.5	−17.2	−17.8
CAM-B3LYP	−18.5	−17.3	−17.8
M11	−18.6	**−17.0**	−17.9
M062X-D	−19.3	−17.4	−17.9
B3LYP-D	−19.7	−17.5	−18.0
PBE0-D	−19.9	−17.2	−17.8
CAM-B3LYP-D	**−21.1**	−17.4	−17.8
MP2/av(D+d)z	−17.7	−17.3	**−18.2**
MP2/av(T+d)z	−18.8	−17.5	−18.0

[a]Values are presented in kcal/mol.

The DLPNO method is observed to underbind compared with canonical coupled cluster, with a mean absolute error of 0.6 kcal/mol and with the largest deviation being 0.9 kcal/mol. Using a single functional (M06-2X) to obtain the geometries, the DLPNO method was tested against F12 for reactions 1−6. We obtain a MAE of 0.4 kcal/mol with a maximum error of 0.8 kcal/mol for the $(H_2SO_4)((CH_3)_2NH)$ complex. Interestingly, the underbinding of the DLPNO method is consistent, which is not the case for the DFT functionals, where the sign of the error is very dependent on the reaction at hand. This indicates that the DLPNO calculation can be used as a lower bound for the "true" canonical coupled cluster binding energy.

3.2. Extensions to Medium Sized Clusters. To extend the usage of the DLPNO method to larger clusters, we compare it with canonical coupled cluster methods for medium-sized systems. The binding energies of $(H_2SO_4)_{1-2}(NH_3)_{1-2}$ and $(H_2SO_4)_{1-2}((CH_3)_2NH)_{1-2}$ clusters are presented in Table 3. The geometries were extracted from Ortega et al.[46] and have been re-evaluated using the M06-2X functional. The structures obtained in the work of Ortega et al. represent several years of intensive configurational sampling of the system, and thereby no further sampling was conducted.

While very similar in construction, we substitute the 6-311++G(3df,3pd) basis set with MG3S because it has been widely used together with the M06-2X functional. Using the VDZ-F12 basis set allowed calculations on clusters up to $(H_2SO_4)_2(NH_3)_2$, with the $(H_2SO_4)_2((CH_3)_2NH)_2$ cluster being too large. DLPNO calculations were easily performed on all the medium-sized systems.

The binding energy calculated using the DLPNO method underbinds compared with canonical coupled cluster methods, which is consistent with the trends identified for the smaller complexes. The MAE between the canonical and local coupled cluster method is 1.3 kcal/mol, with a maximum error of 2.4 kcal/mol for the $(H_2SO_4)_2(NH_3)_2$ cluster. The M06-2X/MG3S binding energies overbind compared with the explicitly correlated coupled cluster results and yield a MAE of 1.3 kcal/mol, with the largest variation up to 2.8 kcal/mol, as seen for the (H_2SO_4) $(NH_3)_2$ cluster. Although the MAE for M06-2X/MG3S and DLPNO is identical, the error in the DLPNO binding energy is seen to increase with increasing system size, whereas the M06-2X/MG3S errors appear to be more random. This could indicate that the DLPNO error is a systematic underestimation. The ratio between the F12/DLPNO results is found to be in the range of 1.01 to 1.04, with a mean ratio of 1.03. By scaling the DLPNO results by this factor the MAE is reduced from 1.3 to 0.3 kcal/mol, with a maximum error of 0.5 kcal/mol. This indicates that the DLPNO method is an attractive choice for calculating the binding energies of atmospheric molecular clusters, as the results are more systematic than those of DFT methods. The scaling factor of 1.03 derived here should not be used as a global scaling factor, as different systems behave differently in this respect. We recently identified that the ratio between the F12/DLPNO results for clusters consisting of highly oxidized ketodiperoxy acids and sulfuric acid would yield a scaling factor of 1.10.[40]

Table 3. Binding Energies Calculated Using M06-2X/MG3S and Coupled Cluster Methods[a]

method basis set	F12 VDZ-F12	def2-QZVPP	M06-2X MG3S	$\Delta_{DLPNO-F12}$	$\Delta_{DFT-F12}$
(H_2SO_4) (NH_3)	−16.1	−15.9	−17.8	0.2	−1.7
$(H_2SO_4)((CH_3)_2NH)$	−23.7	−22.9	−23.6	0.8	0.1
(H_2SO_4) $(NH_3)_2$	−30.6	−30.0	−33.4	0.6	−2.8
$(H_2SO_4)((CH_3)_2NH)_2$	−38.2	−36.6	−39.7	1.6	−1.5
$(H_2SO_4)_2(NH_3)$	−45.1	−43.5	−46.4	1.6	−1.3
$(H_2SO_4)_2((CH_3)_2NH)$	−56.8	−55.0	−57.3	1.8	−0.5
$(H_2SO_4)_2(NH_3)_2$	−64.6	−62.2	−65.9	2.4	−1.3
$(H_2SO_4)_2((CH_3)_2NH)_2$		−82.9	−87.0		

[a]All geometries have been obtained at the M06-2X/MG3S level of theory. The values are presented in kcal/mol.

DOI: 10.1021/acs.jpca.5b09762
J. Phys. Chem. A 2016, 120, 621−630

3.3. Extension to Large Clusters. In the previous two sections it was shown that the DLPNO method significantly reduces the potential scatter in the binding energies, which are present in DFT calculations. Furthermore, the DLPNO method consistently underbinds compared with canonical coupled cluster, which indicates that the binding energies can be used as a lower bound. We now extend the calculations to large $(H_2SO_4)_{1-5}(NH_3)_{1-5}$ and $(H_2SO_4)_{1-4}((CH_3)_2NH)_{1-5}$ clusters. All of the clusters have been extracted from the work by Ortega et al.[46] and Figure 1 shows the Gibbs free binding energies of these clusters.

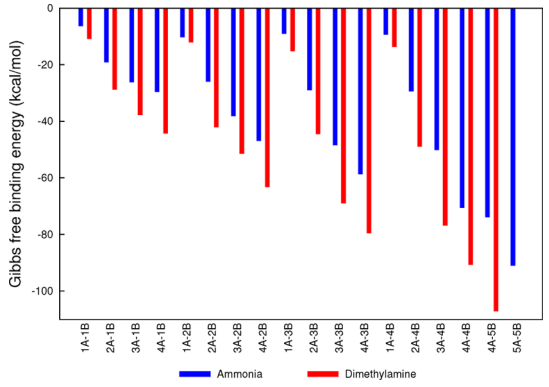

Figure 1. Gibbs free binding energies of $(H_2SO_4)_{1-5}(NH_3)_{1-5}$ and $(H_2SO_4)_{1-4}((CH_3)_2NH)_{1-5}$ clusters, calculated at the DLPNO-CCSD(T)/def2-QZVPP//M06-2X/MG3S level of theory.

The Gibbs free binding energies are very dependent on several factors, most importantly the temperature and the treatment of electron correlation used to evaluate the binding energies. For the Gibbs free energy the effect of lowering the temperature from 298 to 278 K and including perturbative triples (T) in the treatment of electron correlation is shown in Figure 2. The temperature variation illustrates how ΔG values vary with the conditions, while the inclusion of (T) illustrates the sensitivity of the values toward the electron correlation treatment. The values are reported relative to the DLPNO values shown in Figure 1. Previously, the potential energy surface of the $(H_2SO_4)_{1-5}(NH_3)_{1-5}$ and $(H_2SO_4)_{1-4}((CH_3)_2NH)_{1-5}$ clusters has been evaluated using RI-CC2/aug-cc-pV(T+d)Z binding energies calculated on top of B3LYP/CBSB7 geometries, denoted B3RICC2.[46] The effect of using B3RICC2 instead of DLPNO//M06-2X/MG3S is also shown in Figure 2a for ammonia and Figure 2b for dimethylamine.

Lowering the temperature from 298 to 278 K, the formation free energies are seen to be up to 6.4 kcal/mol more favorable. On average the lower temperature leads to 11 and 8% more favorable binding free energies for the ammonia and dimethylamine containing clusters, respectively. It is well known that new particle formation is accompanied by a decrease in the entropy and thereby leads to more favorable Gibbs free energies as the temperature decreases.[1]

The binding energies have been calculated at both the DLPNO-CCSD and DLPNO-CCSD(T) level of theory to illustrate the importance of the perturbative triples for these large clusters. The triples contribution accounts for up to 5.9 kcal/mol in the Gibbs free energy. This further emphasizes that perturbative triples are essential when utilizing coupled cluster methods to study atmospheric molecular clusters. The effect of including perturbative triples and changing the temperature from 298 to 278 K is similar in magnitude.

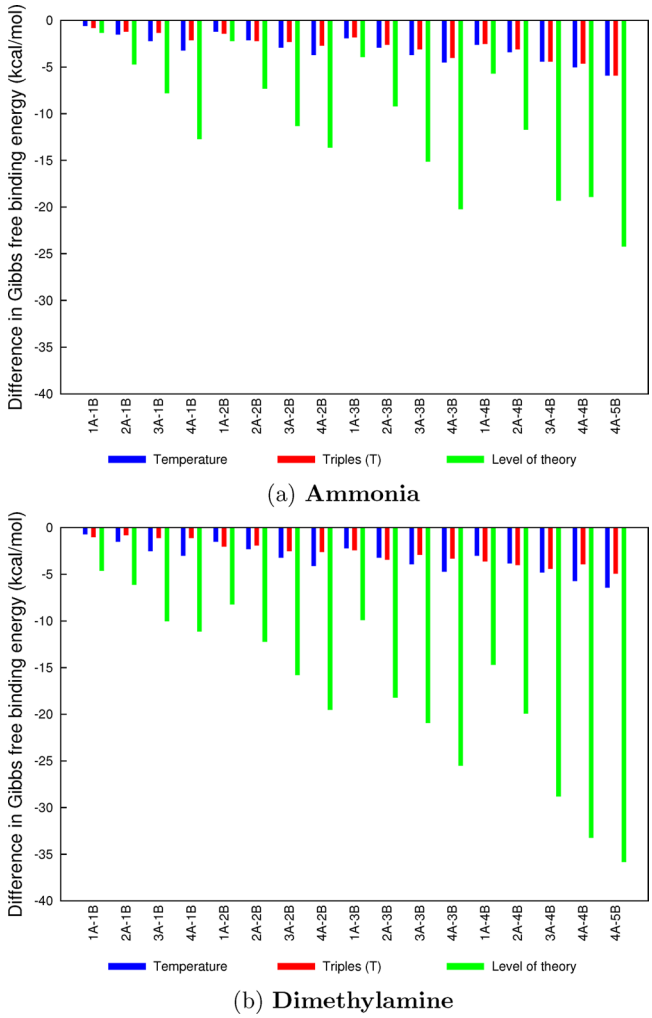

Figure 2. Illustration of the sensitivity of ΔG on the conditions and the calculation method. The effect of changing the temperature from 298 to 278 K is shown in blue. The effect of including perturbative triples are shown in red. The effect of using the RI-CC2/aug-cc-pV(T+d)Z//B3LYP/CBSB7 level of theory is shown in green. All values are in kcal/mol and are shown relative to DLPNO results.

As established in previous sections, the DLPNO method is underestimating the binding energies. Previously, the B3RICC2 method has been used to calculate the binding free energies of sulfuric acid−ammonia and sulfuric acid−dimethylamine clusters. It has, however, been established that B3RICC2 overestimate the binding energies compared with high-level explicitly correlated coupled cluster.[56] Figure 2 shows the difference between the DLPNO and B3RICC2 calculated Gibbs free energies. The B3RICC2 Gibbs free energies are significantly more negative than DLPNO, by up to 35.8 kcal/mol. The effect of the level of theory used to obtain the binding energy influences the Gibbs free energy significantly more than changing the temperature and including triples corrections. Because of the higher accuracy of the DLPNO method, the DLPNO binding energies should be significant more reliable than the B3RICC2 values. In Section 3.2 it was found that applying a scaling factor of 1.03 to the DLPNO binding energy yielded significantly better agreement with the explicitly correlated canonical coupled cluster values. After applying

DOI: 10.1021/acs.jpca.5b09762
J. Phys. Chem. A 2016, 120, 621−630

this scaling factor, the resulting Gibbs free energy values should represent a reliable measure close to the real CCSD(T)-F12a/VDZ-F12 value. The unscaled and scaled DLPNO Gibbs free energy values are plotted alongside B3RICC2 results in Figure 3a for ammonia and Figure 3b for dimethylamine.

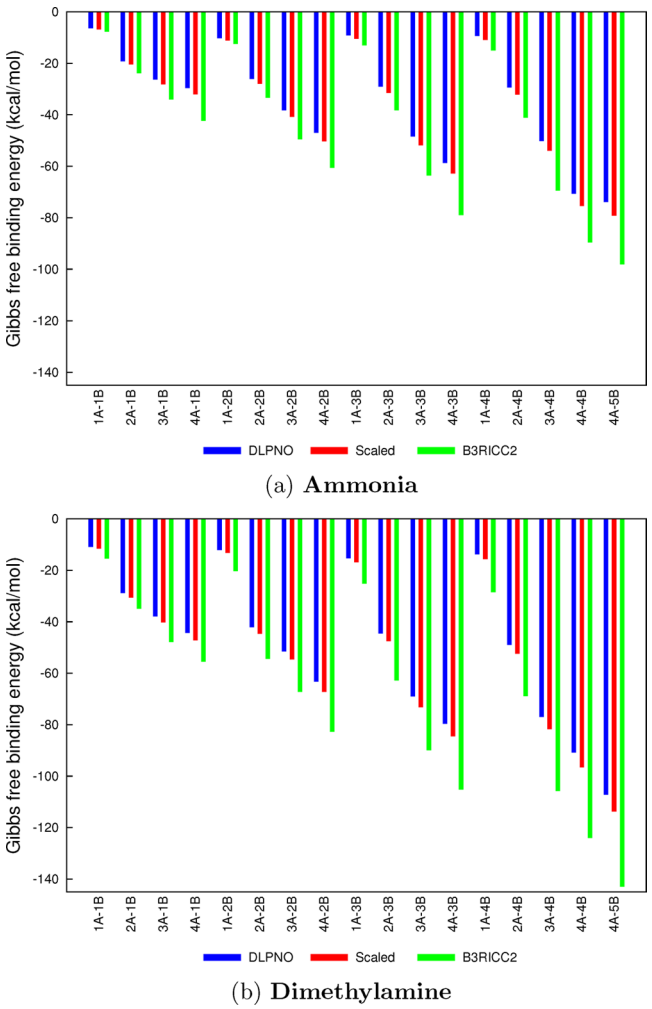

Figure 3. Gibbs free binding energy depending on computational method used. DLPNO (blue), DLPNO scaled by 1.03 (red), and B3RICC2 (green). Values are in kcal/mol.

While the scaling factor makes the cluster formation free energies more favorable, the values are still significantly less favorable than the B3RICC2 values. It should be mentioned that a new configurational sampling has not been performed, so the clusters may not represent a global minimum on the DLPNO//M06-2X/MG3S potential energy surface. This implies that we obtain a lower bound for the stability and thereby an upper bound for the ΔG value. Other effects such as conformational and vibrational anharmonicity, extrapolation to the complete basis set limit, and hydration could also all make the cluster formation free energies more negative. Test calculations on basis set effects were carried out by extrapolation to the complete basis set limit (3−4 extrapolation) and indicated a minor difference of <1 kcal/mol. Tests on different conformations of the $(H_2SO_4)_3(NH_3)_3$ cluster indicated that conformational sampling could yield a lowering of up to 3.8 kcal/mol in the binding energy. Assuming that the effect of conformational sampling scales with system size, which is reasonable considering the exponentially increasing amount of local minima, large clusters consisting of 10 molecules could thus easily be affected by up to ∼6 kcal/mol. Previous studies on hydration of acid−base clusters have shown that the maximum achievable effective stabilization caused by hydration is on the order of ∼2 kcal/mol.[69] The effective stabilization was evaluated using the difference of acid or base evaporation rates at RH 0% and RH 100%. It should be noted that in terms of the evaporation rates, many clusters are actually destabilized rather than stabilized by hydration. The role of anharmonicity has previously been studied for water clusters, where it was found that the energetic ordering of the isomers were unaffected, but the formation free energy was lowered by ∼0.4 kcal/mol per water molecule in a 10-water cluster.[70] This indicates that the collective effect of all of these contributions could make the formation free energies of the largest clusters significantly more negative. As a rough estimate for a cluster consisting of 10 molecules this would add up to ∼13 kcal/mol (1 kcal/mol for the basis set extrapolation, 6 kcal/mol from configurational sampling, 4 kcal/mol for anharmonicity, and 2 kcal/mol for hydration). While a significant change, it is worth noting that even this estimate is significantly smaller than the difference between DLPNO and B3RICC2 results for the largest clusters.

3.4. Comparison with Dimer Formation Experiments.

The formation of sulfuric acid dimers has been shown to be an important initial step in the formation of new particles.[47] To estimate the applicability of the DLPNO method, we compared the calculations with the CLOUD chamber experiments at CERN[17] and the flow tube measurements of Jen et al.[71]

The total concentration of sulfuric acid "dimers" (defined as the sum of the concentrations of all clusters containing two sulfuric acid molecules and any number of stabilizing water and/or base molecules) has been measured as a function of both the sulfuric acid monomer concentration and the base concentration. Note that the concentration measurement is performed by chemical ionization mass spectrometry, which results in the loss of almost all stabilizer molecules prior to detection of the dimers as $(HSO_4^-)(H_2SO_4)$.[72] These measurements can be compared with the dimer concentration predicted by the Atmospheric Cluster Dynamics Code (ACDC) code[73] using either the scaled DLPNO or the B3RICC free energies as input. In brief, the model solves the time evolution of the cluster concentrations by using the estimated rates of the evaporation and condensation processes of the clusters. The used model is described in detail by McGrath et al.[73] and Olenius et al.[74] For comparison with the dimer data of the CLOUD measurements at CERN,[17] the simulated concentrations should reach a steady state ; that is, the concentrations are converged with time. (See Figure 4a for ammonia and Figure 4b for dimethylamine.) Also, the monomer concentrations for acid and base are kept constant during the simulation. The measurement by Jen et al.[71] has a well-defined reaction time of 3 s and in the simulation the monomer concentrations are let to evolve during the run (see Figure 5a for ammonia and Figure 5 for dimethylamine). The studied neutral clusters have primary clustering pathway along the diagonal on an acid−base grid; that is, the clusters with an equal amount of acid and base molecules are the most stable products.[47] The simulation system has a finite size and clusters with a certain composition are allowed to leave the system so that they cannot evaporate back into the system. For the ammonia system, clusters containing five acids and four bases are allowed to leave the system, while this is limited to four

DOI: 10.1021/acs.jpca.5b09762
J. Phys. Chem. A 2016, 120, 621−630

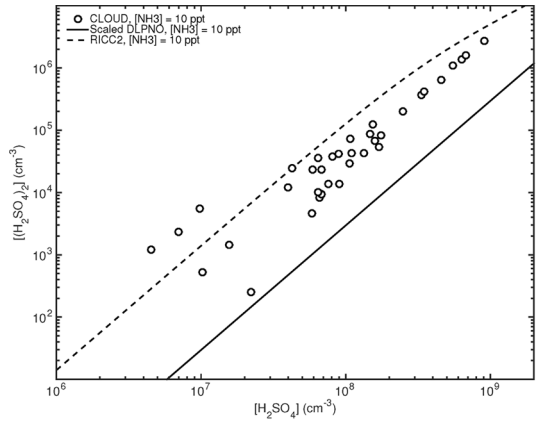

(a) **Ammonia**

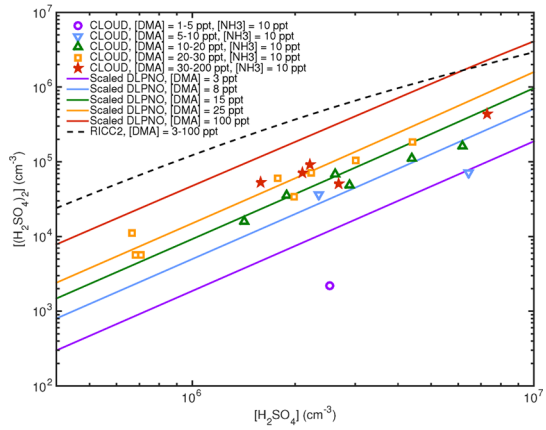

(b) **Dimethylamine**

Figure 4. (a) Modeled steady-state sulfuric acid dimer concentration as a function of ammonia concentration of 10 ppt and (b) dimethylamine concentration in the range of 3 to 100 ppt at 278 K. The solid lines show the scaled DLPNO results, while the dashed lines show the B3RICC2 results. The points are experimental data obtained at the CLOUD chamber.

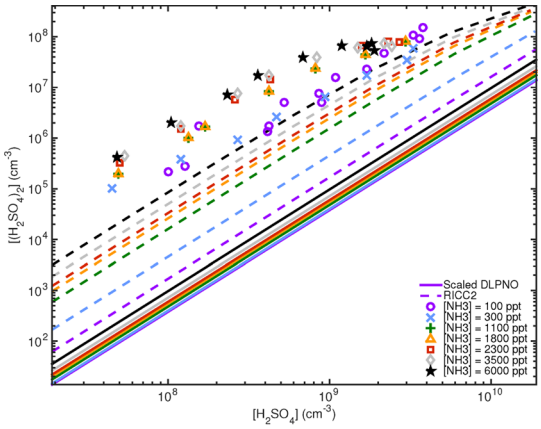

(a) **Ammonia**

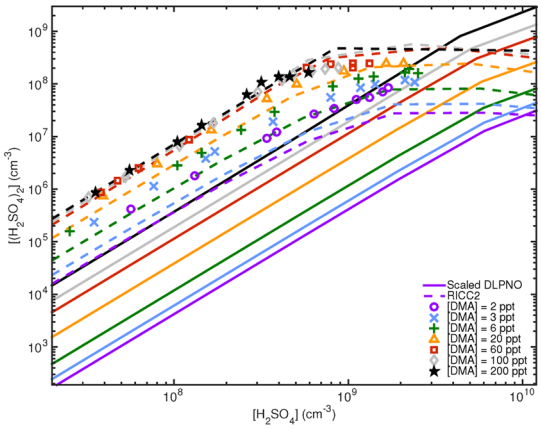

(b) **Dimethylamine**

Figure 5. (a) Modeled sulfuric acid dimer concentration as a function of ammonia concentration in the range of 100 ppt to 6 ppb and (b) dimethylamine concentration in the range of 2 to 200 ppt at 298.15 K. The solid lines show the scaled DLPNO results, while the dashed lines show the B3RICC2 results. The points are experimental data for the corresponding base concentrations obtained at the flow tube experiment of Jen et al.

acids and five base molecules for dimethylamine containing clusters. The largest off-diagonal clusters are evaporated back into the system by arbitrary removal of the weakest bound molecule. In the model, other processes besides evaporation and condensation are also taken into account as follows. In the CLOUD experiment, two sink terms are reported: dilution sink and wall loss of clusters. The dilution sink is set to a constant value of 1.06×10^{-4} s^{-1} and the wall loss factor is size-dependent and it has been parametrized for neutral clusters. For the measurements in Jen et al., only a diffusion limited wall loss for a cylindrical flow tube is implemented in the model, as described in detail by Olenius et al.[75] It is worth noting that all of the simulations are done for dry clusters (RH = 0%) and the sticking factor for all collisions was set to 1.

Figure 4a shows that the DLPNO energies, even after scaling, predict lower formation of sulfuric acid dimers than both B3RICC2 and the experiments performed at the CLOUD chamber for ammonia clusters. The agreement is significantly better for dimethylamine in Figure 4b, where DLPNO is seen to be close to the experimental data, while B3RICC2 overestimates the dimer formation. In Figure 5a the dimer formation for ammonia containing clusters can be seen compared with the flow tube experiments by Jen et al.

The DLPNO energies predict significantly lower formation of sulfuric acid dimers than both B3RICC2, and the experiments performed in the flow tube experiments by Jen et al. for both ammonia (Figure 5a) and dimethylamine (Figure 5b).

For dimethylamine clusters the DLPNO method is seen to reproduce the CLOUD data significantly better than the flow tube experiments. This could indicate that we well reproduce the steady-state conditions but get a worse result for the kinetics. To further investigate this discrepancy, we look into the time evolution of the cluster concentrations in the flow tube experiments using dimethylamine clusters with an initial dimethylamine concentration of 20 ppt. Figure 6 shows $\frac{d[2A1D]}{dt}$ as a function of reaction time (top panel) and the concentration as a function of reaction time for 2A1D, 2A, 1A1D clusters and 1A, 1D monomers (bottom panel) for both DLPNO and RI-CC2. The initial sulfuric acid concentration is set to 10^9 cm^{-3} in the simulations.

For DLPNO the $\frac{d[2A1D]}{dt}$ value decreases monotonically, whereas there is seen a peak in the RI-CC2 value around 1.5 s.

DOI: 10.1021/acs.jpca.5b09762
J. Phys. Chem. A 2016, 120, 621−630

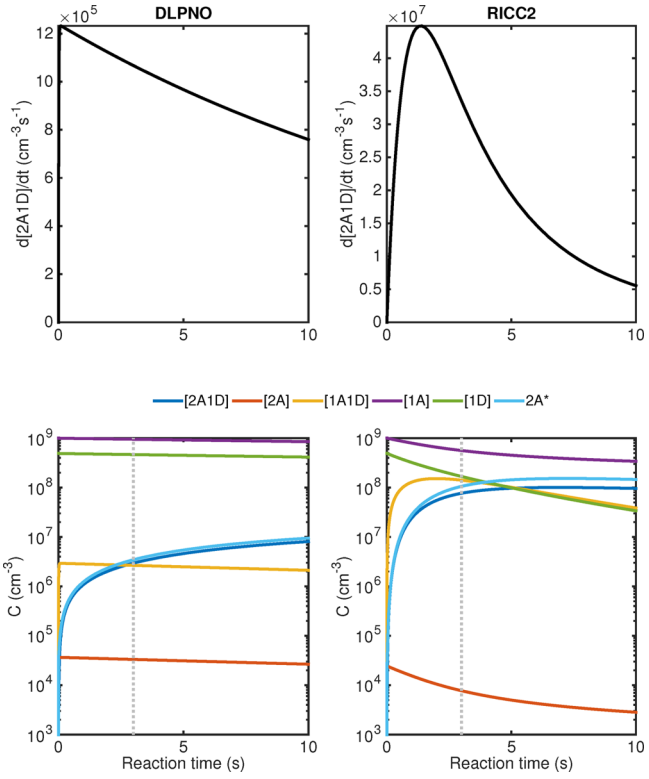

Figure 6. $\frac{d[2A1D]}{dt}$ as a function of reaction time (top panel) and the concentration as a function of reaction time for 2A1D, 2A, 1A1D clusters and 1A, 1D monomers (bottom panel) calculated using DLPNO (left) and RICC2 (right). The initial sulfuric acid (1A) concentration is set to 10^9 cm^{-3}, and the initial dimethylamine (1D) concentration is set to 20 ppt.

The 1A1D cluster quickly reaches a steady-state value in the DLPNO simulations as opposed to the RI-CC2 simulations; however, the steady-state value is quite low. The faster buildup of dimers in the RI-CC2 simulations is thereby due to the depletion of the monomers, as they flow through the 1A1D cluster. To further confirm that the discrepancy between the DLPNO and RI-CC2 results is mainly due to the formation of the 1A1D cluster, we manually changed the formation free-energy value. By changing the DLPNOs 1A1D values to correspond RI-CC2, the comparison with the flow tube data is much better, but at high DMA concentrations the prediction begin to diverge. By keeping all other values fixed and iteratively changing the 1A1D ΔG value, a value of −12.5 kcal/mol yielded good results for DLPNO compared with the flow tube experiments; however, this modification did simultaneously make the results in slightly worse agreement with the CLOUD chamber data. This does, however, further indicate that the formation of dimers is highly dependent on the stability of the 1A1D complex. The DLPNO method will thereby severely underpredict the formation rate of sulfuric acid-based clusters under atmospheric conditions. This is perhaps not entirely surprising, as the DLPNO binding energies (and especially free energies) reported here are expected to represent a lower limit. Nevertheless, from a theoretical point of view the DLPNO method represents a significantly more advanced and accurate treatment of electron correlation than the RI-CC2 method, indicating that the remaining errors arise mainly from other factors than the actual binding energy (electronic energy). Including effects from hydration, conformational sampling, anharmonicity, and basis set extrapolation would yield a better agreement between DLPNO and the experimental results. On the contrary, including effects such as hydration and anharmonicity within the B3RICC2 method would likely make the agreement with experiments performed either at the CLOUD chamber or the flow tube measurements worse.

The identification that the dimer formation is mainly dependent on the stability of the 1A1D complex makes it crucial that the ΔG value for this complex is determined very accurately. Currently, to our knowledge the most accurate literature estimate is obtained at CCSD(T)-F12a/VDZ-F12 calculated on top of geometries obtained with DFT using a 6-311++G(3df,3pd) basis set. A value between −11.26 and −11.99 kcal/mol was obtained depending on whether the M06-2X, PW91, or ωB97X-D functional was used to obtain the geometry and thermal correction to the free energy.[56] Determining the formation free energy of the 1A1D complex experimentally or by means of highly accurate calculations (including effects from both anharmonicity and hydration) would be very valuable as this complex appears to be the key uncertainty for accurately simulating dimer formation experiments.

4. CONCLUSIONS

A systematic comparison of the performance of increasingly accurate methods is essential for achieving accuracy that allows reproducing and predicting atmospheric particle formation. We have investigated the applicability of the DLPNO-CCSD(T) method for calculating the binding energies of atmospherically relevant molecular clusters. We find a large scatter in the binding energy between different applied DFT methods with variations up to 4.0 kcal/mol for small atmospheric complexes. Applying the DLPNO method, the variation was significantly reduced to 0.6 kcal/mol. Extending to medium sized clusters where canonical methods are still applicable we found that the DLPNO method yields significantly more consistent results than DFT. Furthermore, the DLPNO binding energies were found to systematically underbind compared with F12 results, which indicates that the obtained values can be used as a lower bound. The DLPNO results were found to be systematically dependent on cluster size, indicating that a scaling factor can be applied to allow better correlation with canonical coupled cluster results. Using these findings we extended the DLPNO calculations to large sulfuric acid−base clusters consisting of up to 10 molecules. On the basis of the scaled DLPNO binding energies, ACDC simulations predicted sulfuric acid dimer concentrations to be significantly lower than experimental results. Although in worse agreement with flow tube experiments, the DLPNO binding energy results should be more reliable than RI-CC2, as they come from a higher level of theory. The remaining errors are assumed to arise from other effects such as anharmonicity, extrapolation to the complete basis set limit, different global minima, and hydration. The combined findings over the investigated three size ranges indicate that the DLPNO method is an attractive choice to calculate the binding energy of atmospheric molecular clusters and can easily be used as a more reliable substitute for routine DFT binding energy calculations.

DOI: 10.1021/acs.jpca.5b09762
J. Phys. Chem. A 2016, 120, 621−630

■ ASSOCIATED CONTENT

Supporting Information

The Supporting Information is available free of charge on the ACS Publications website at DOI: 10.1021/acs.jpca.5b09762.

All calculated binding energies. (PDF)

■ AUTHOR INFORMATION

Corresponding Author

*E-mail: jonas.elm@helsinki.fi. Tel: +45 28938085.

Notes

The authors declare no competing financial interest.

■ ACKNOWLEDGMENTS

We thank Oona Kupiainen-Määttä for assistance with ACDC. We thank Academy of Finland and ERC project 257360-MOCAPAF for funding and CSC for computer resources. J.E. thanks the Carlsberg Foundation for financial support and the Danish e-Infrastructure Cooperation (DeIC) for computing time.

■ REFERENCES

(1) Zhang, R.; Khalizov, A.; Wang, L.; Hu, M.; Xu, W. Nucleation and Growth of Nanoparticles in the Atmosphere. *Chem. Rev.* **2012**, *112*, 1957−2011.

(2) Kulmala, M.; Kontkanen, J.; Junninen, H.; Lehtipalo, K.; Manninen, H. E.; Nieminen, T.; Petäjä, T.; Sipilä, M.; Schobesberger, S.; Rantala, P.; et al. Direct Observations of Atmospheric Aerosol Nucleation. *Science* **2013**, *339*, 943−946.

(3) Kurtén, T.; Sundberg, M. R.; Vehkamäki, H.; Noppel, M.; Blomqvist, J.; Kulmala, M. Ab Initio and Density Functional Theory Reinvestigation of Gas-Phase Sulfuric Acid Monohydrate and Ammonium Hydrogen Sulfate. *J. Phys. Chem. A* **2006**, *110*, 7178−7188.

(4) Kurtén, T.; Torpo, L.; Sundberg, M. R.; Kerminen, V.; Vehkamäki, H.; Kulmala, M. Estimating the NH_3:H_2SO_4 Ratio of Nucleating Clusters in Atmospheric Conditions using Quantum Chemical Methods. *Atmos. Chem. Phys.* **2007**, *7*, 2765−2773.

(5) Kurtén, T.; Torpo, L.; Ding, C.; Vehkamäki, H.; Sundberg, M. R.; Laasonen, K.; Kulmala, M. A Density Functional Study on Water-Sulfuric Acid-ammonia Clusters and Implications for Atmospheric Cluster Formation. *J. Geophys. Res.* **2007**, *112*, D04210.

(6) Herb, J.; Nadykto, A. B.; Yu, F. Large Ternary Hydrogen-bonded Pre-nucleation Clusters in the Earth's Atmosphere. *Chem. Phys. Lett.* **2011**, *518*, 7−14.

(7) DePalma, J. W.; Bzdek, B. R.; Doren, D. J.; Johnston, M. V. Structure and Energetics of Nanometer Size Clusters of Sulfuric Acid with Ammonia and Dimethylamine. *J. Phys. Chem. A* **2012**, *116*, 1030−1040.

(8) DePalma, J. W.; Doren, D. J.; Johnston, M. V. Formation and Growth of Molecular Clusters Containing Sulfuric Acid, Water, Ammonia, and Dimethylamine. *J. Phys. Chem. A* **2014**, *118*, 5464−5473.

(9) Kurtén, T.; Loukonen, V.; Vehkamäki, H.; Kulmala, M. Amines are Likely to Enhance Neutral and Ion-induced Sulfuric Acid-water Nucleation in the Atmosphere More Effectively than Ammonia. *Atmos. Chem. Phys.* **2008**, *8*, 4095−4103.

(10) Kurtén, T.; Ortega, I. K.; Vehkamäki, H. The Sign Preference in Sulfuric Acid Nucleation. *J. Mol. Struct.: THEOCHEM* **2009**, *901*, 169−173.

(11) Loukonen, V.; Kurtén, T.; Ortega, I. K.; Vehkamäki, H.; Pádua, A. A. H.; Sellegri, K.; Kulmala, M. Enhancing Effect of Dimethylamine in Sulfuric Acid Nucleation in the Presence of Water - A Computational Study. *Atmos. Chem. Phys.* **2010**, *10*, 4961−4974.

(12) Nadykto, A. B.; Yu, F.; Jakovleva, M. V.; Herb, J.; Xu, Y. Amines in the Earth's Atmosphere: A Density Functional Theory Study of the Thermochemistry of Pre-Nucleation Clusters. *Entropy* **2011**, *13*, 554−569.

(13) Paasonen, P.; Olenius, T.; Kupiainen, O.; Kurtén, T.; Petäjä, T.; Birmili, W.; Hamed, A.; Hu, M.; Huey, L. G.; Plass-Duelmer, C.; et al. On the Formation of Sulphuric Acid - Amine Clusters in Varying Atmospheric Conditions and its Influence on Atmospheric New Particle Formation. *Atmos. Chem. Phys.* **2012**, *12*, 9113−9133.

(14) Ryding, M. J.; Ruusuvuori, K.; Andersson, P. U.; Zatula, A. S.; McGrath, M. J.; Kurtén, T.; Ortega, I. K.; Vehkamäki, H.; Uggerud, E. Structural Rearrangements and Magic Numbers in Reactions between Pyridine-Containing Water Clusters and Ammonia. *J. Phys. Chem. A* **2012**, *116*, 4902−4908.

(15) Kupiainen, O.; Ortega, I. K.; Kurtén, T.; Vehkamäki, H. Amine Substitution into Sulfuric Acid - Ammonia Clusters. *Atmos. Chem. Phys.* **2012**, *12*, 3591−3599.

(16) Bork, N.; Elm, J.; Olenius, T.; Vehkamäki, H. Methane Sulfonic Acid-Enhanced Formation of Molecular Clusters of Sulfuric Acid and Dimethyl Amine. *Atmos. Chem. Phys.* **2014**, *14*, 12023−12030.

(17) Almeida, J.; Schobesberger, S.; Kurten, A.; Ortega, I. K.; Kupiainen-Määttä, O.; Praplan, A. P.; Adamov, A.; Amorim, A.; Bianchi, F.; Breitenlechner, M.; et al. Molecular Understanding of Sulphuric Acid-Amine Particle Nucleation in the Atmosphere. *Nature* **2013**, *502*, 359−363.

(18) Kürten, A.; Jokinen, T.; Simon, M.; Sipilä, M.; Sarnela, N.; Junninen, H.; Adamov, A.; Almeida, J.; Amorim, A.; Bianchi, F.; et al. Neutral Molecular Cluster Formation of Sulfuric Acid-Dimethylamine Observed in Real Time under Atmospheric Conditions. *Proc. Natl. Acad. Sci. U. S. A.* **2014**, *111*, 15019.

(19) Nadykto, A. B.; Herb, J.; Yu, F.; Xu, Y. Enhancement in the Production of Nucleating Clusters due to Dimethylamine and Large Uncertainties in the Thermochemistry of Amine-Enhanced Nucleation. *Chem. Phys. Lett.* **2014**, *609*, 42−49.

(20) Nadykto, A. B.; Herb, J.; Yu, F.; Xu, Y.; Nazarenko, E. S. Estimating the Lower Limit of the Impact of Amines on Nucleation in the Earth's Atmosphere. *Entropy* **2015**, *17*, 2764−2780.

(21) Lv, S.; Liu, Y.; Huang, T.; Feng, Y.; Jiang, S.; Huang, W. Stability of Hydrated Methylamine: Structural Characteristics and $H_2N \cdots HO$ Hydrogen Bonds. *J. Phys. Chem. A* **2015**, *119*, 3770−3779.

(22) Schobesberger, S.; Junninen, H.; Bianchi, F.; Lönn, G.; Ehn, M.; Lehtipalo, K.; Dommen, J.; Ehrhart, S.; Ortega, I. K.; Franchin, A.; et al. Molecular Understanding of Atmospheric Particle Formation from Sulfuric Acid and Large Oxidized Organic Molecules. *Proc. Natl. Acad. Sci. U. S. A.* **2013**, *110*, 17223−17228.

(23) Metzger, A.; Verheggen, B.; Dommen, J.; Duplissy, J.; Prevot, A. S. H.; Weingartner, E.; Riipinen, I.; Kulmala, M.; Spracklen, D. V.; Carslaw, K. S.; et al. Evidence for the Role of Organics in Aerosol Particle Formation under Atmospheric Conditions. *Proc. Natl. Acad. Sci. U. S. A.* **2010**, *107*, 6646−6651.

(24) Zhang, R. Getting to the Critical Nucleaus of Aerosol Formation. *Science* **2010**, *328*, 1366−1367.

(25) Zhang, R.; Suh, I.; Zhao, J.; Zhang, D.; Fortner, E. C.; Tie, X.; Molina, L. T.; Molina, M. J. Atmospheric New Particle Formation Enhanced by Organic Acids. *Science* **2004**, *304*, 1487−1490.

(26) Christoffersen, T.; Hjorth, J.; Horie, O.; Jensen, N.; Kotzias, D.; Molander, L. L.; Neeb, P.; Ruppert, L.; Winterhalter, R.; Virkkula, A.; et al. Cis-Pinic Acid, a Possible Precursor for Organic Aerosol Formation from Ozonolysis of α-Pinene. *Atmos. Environ.* **1998**, *32*, 1657−1661.

(27) McFiggans, G. Involatile Particles from Rapid Oxidation. *Nature* **2014**, *506*, 442−443.

(28) Ehn, M.; Thornton, J. A.; Kleist, E.; Sipilä, M.; Junninen, H.; Pullinen, I.; Springer, M.; Rubach, F.; Tillmann, R.; Lee, B.; et al. A Large Source of Low-Volatility Secondary Organic Aerosol. *Nature* **2014**, *506*, 476−479.

(29) Xu, Y.; Nadykto, A. B.; Yu, F.; Jiang, L.; Wang, W. Formation and Properties of Hydrogen-bonded Complexes of Common Organic Oxalic Acid with Atmospheric Nucleation Precursors. *J. Mol. Struct.: THEOCHEM* **2010**, *951*, 28−33.

(30) Nadykto, A. B.; Yu, F. Strong Hydrogen Bonding between Atmospheric Nucleation Precursors and Common Organics. *Chem. Phys. Lett.* **2007**, *435*, 14−18.
(31) Elm, J.; Bilde, M.; Mikkelsen, K. V. Influence of Nucleation Precursors on the Reaction Kinetics of Methanol with the OH Radical. *J. Phys. Chem. A* **2013**, *117*, 6695−6701.
(32) Xu, W.; Zhang, R. Theoretical Investigation of Interaction of Dicarboxylic Acids with Common Aerosol Nucleation Precursors. *J. Phys. Chem. A* **2012**, *116*, 4539−4550.
(33) Xu, Y.; Nadykto, A. B.; Yu, F.; Herb, J.; Wang, W. Interaction between Common Organic Acids and Trace Nucleation Species in the Earth's Atmosphere. *J. Phys. Chem. A* **2010**, *114*, 387−396.
(34) Zhao, J.; Khalizov, A.; Zhang, R.; McGraw, R. L. Hydrogen-Bonding Interaction in Molecular Complexes and Clusters of Aerosol Nucleation Precursors. *J. Phys. Chem. A* **2009**, *113*, 680−689.
(35) Elm, J.; Fard, M.; Bilde, M.; Mikkelsen, K. V. Interaction of Glycine with Common Atmospheric Nucleation Precursors. *J. Phys. Chem. A* **2013**, *117*, 12990−12997.
(36) Zhang, R.; Suh, I.; Zhao, J.; Zhang, D.; Fortner, E. C.; Tie, X.; Molina, L. T.; Molina, M. J. Atmospheric New Particle Formation Enhanced by Organic Acids. *Science* **2004**, *304*, 1487−1490.
(37) Zhang, R.; Wang, L.; Khalizov, A. F.; Zhao, J.; Zheng, J.; McGraw, R. L.; Molina, L. T. Formation of Nanoparticles of Blue Haze Enhanced by Anthropogenic Pollution. *Proc. Natl. Acad. Sci. U. S. A.* **2009**, *106*, 17650−17654.
(38) Riccobono, F.; Schobesberger, S.; Scott, C. E.; Dommen, J.; Ortega, I. K.; Rondo, L.; Almeida, J.; Amorim, A.; Bianchi, F.; Breitenlechner, M.; et al. Oxidation Products of Biogenic Emissions Contribute to Nucleation of Atmospheric Particles. *Science* **2014**, *344*, 717−721.
(39) Elm, J.; Kurtén, T.; Bilde, M.; Mikkelsen, K. V. Molecular Interaction of Pinic Acid with Sulfuric Acid - Exploring the Thermodynamic Landscape of Cluster Growth. *J. Phys. Chem. A* **2014**, *118*, 7892−7900.
(40) Elm, J.; Myllys, N.; Hyttinen, N.; Kurtén, T. Computational Study of the Clustering of a Cyclohexene Autoxidation Product $C_6H_8O_7$ with Itself and Sulfuric Acid. *J. Phys. Chem. A* **2015**, *119*, 8414−8421.
(41) Weber, K. H.; Morales, F. J.; Tao, F. Theoretical Study on the Structure and Stabilities of Molecular Clusters of Oxalic Acid with Water. *J. Phys. Chem. A* **2012**, *116*, 11601−11617.
(42) Weber, K. H.; Liu, Q.; Tao, F. Theoretical Study on Stable Small Clusters of Oxalic Acid with Ammonia and Water. *J. Phys. Chem. A* **2014**, *118*, 1451−1468.
(43) Peng, X.; Liu, Y.; Huang, T.; Jiang, S.; Huang, W. Interaction of Gas Phase Oxalic Acid with Ammonia and its Atmospheric Implications. *Phys. Chem. Chem. Phys.* **2015**, *17*, 9552−9563.
(44) Miao, S.; Jiang, S.; Chen, J.; Ma, Y.; Zhu, Y.; Wen, Y.; Zhang, M.; Huang, W. Hydration of a Sulfuric Acid - Oxalic Acid Complex: Acid Dissociation and its Atmospheric Implication. *RSC Adv.* **2015**, *5*, 48638−48646.
(45) McGrath, M. J.; Olenius, T.; Ortega, I. K.; Loukonen, V.; Paasonen, P.; Kurtén, T.; Kulmala, M.; Vehkamäki, H. Atmospheric Cluster Dynamics Code: A Flexible Method for Solution of the Birth-Death Equations. *Atmos. Chem. Phys.* **2012**, *12*, 2345−2355.
(46) Ortega, I. K.; Kupiainen, O.; Kurtén, T.; Olenius, T.; Wilkman, O.; McGrath, M. J.; Loukonen, V.; Vehkamäki, H. From Quantum Chemical Formation Free Energies to Evaporation Rates. *Atmos. Chem. Phys.* **2012**, *12*, 225−235.
(47) Olenius, T.; Kupiainen-Määttä, O.; Ortega, I. K.; Kurtén, T.; Vehkamäki, H. Free Energy Barrier in the Growth of Sulfuric Acid-Ammonia and Sulfuric Acid-Dimethylamine Clusters. *J. Chem. Phys.* **2013**, *139*, 084312.
(48) Temelso, B.; Morrell, T. E.; Shields, R. M.; Allodi, M. A.; Wood, E. K.; Kirschner, K. N.; Castonguay, T. C.; Archer, K. A.; Shields, G. C. Quantum Mechanical Study of Sulfuric Acid Hydration: Atmospheric Implications. *J. Phys. Chem. A* **2012**, *116*, 2209−2224.
(49) Temelso, B.; Phan, T. N.; Shields, G. C. Computational Study of the Hydration of Sulfuric Acid Dimers: Implications for Acid Dissociation and Aerosol Formation. *J. Phys. Chem. A* **2012**, *116*, 9745−9758.
(50) Husar, D. E.; Temelso, B.; Ashworth, A. L.; Shields, G. C. Hydration of the Bisulfate Ion: Atmospheric Implications. *J. Phys. Chem. A* **2012**, *116*, 5151−5163.
(51) Bustos, D. J.; Temelso, B.; Shields, G. C. Hydration of the Sulfuric Acid-Methylamine Complex and Implications for Aerosol Formation. *J. Phys. Chem. A* **2014**, *118*, 7430−7441.
(52) Elm, J.; Bilde, M.; Mikkelsen, K. V. Assessment of Density Functional Theory in Predicting Structures and Free Energies of Reaction of Atmospheric Prenucleation Clusters. *J. Chem. Theory Comput.* **2012**, *8*, 2071−2077.
(53) Bork, N.; Du, L.; Kjaergaard, H. G. Identification and Characterization of the HCl-DMS Gas Phase Molecular Complex via Infrared Spectroscopy and Electronic Structure Calculations. *J. Phys. Chem. A* **2014**, *118*, 1384−1389.
(54) Bork, N.; Du, L.; Reiman, H.; Kurtén, T.; Kjaergaard, H. G. Benchmarking Ab Initio Binding Energies of Hydrogen-Bonded Molecular Clusters Based on FTIR Spectroscopy. *J. Phys. Chem. A* **2014**, *118*, 5316−5322.
(55) Elm, J.; Mikkelsen, K. V. Assessment of Binding Energies of Atmopsheric Clusters. *Chem. Phys. Lett.* **2014**, *615*, 26−29.
(56) Elm, J.; Bilde, M.; Mikkelsen, K. V. Computational Approaches for Efficiently Modelling of Small Atmospheric Clusters. *Phys. Chem. Chem. Phys.* **2013**, *15*, 16442−16445.
(57) Feyereisen, M.; Fitzgerald, G.; Komornicki, A. Use of Approximate Integrals in Ab Initio Theory. An Application in MP2 Energy Calculations. *Chem. Phys. Lett.* **1993**, *208*, 359−363.
(58) Rendell, A. P.; Lee, T. J. Coupled Cluster Theory Employing Approximate Integrals: An Approach to Avoid the Input/Output and Storage Bottlenecks. *J. Chem. Phys.* **1994**, *101*, 400.
(59) Werner, H.; Adler, T. B.; Manby, F. R. General Orbital Invariant MP20F12 Theory. *J. Chem. Phys.* **2007**, *126*, 164102.
(60) Adler, T. B.; Knizia, G.; Werner, H. A Simple and Efficient CCSD(T)-F12 Approximation. *J. Chem. Phys.* **2007**, *127*, 221106.
(61) Knizia, G.; Adler, T. B.; Werner, H. Simplified CCSD(T)-F12 Methods: Theory and Benchmarks. *J. Chem. Phys.* **2009**, *130*, 054104.
(62) Riplinger, C.; Neese, F. An Efficient and Near Linear Scaling Pair Natural Orbital Based Local Coupled Cluster Method. *J. Chem. Phys.* **2013**, *138*, 034106.
(63) Riplinger, C.; Sandhoefer, B.; Hansen, A.; Neese, F. Natural Triple Excitations in Local Coupled Cluster Calculations with Pair Natural Orbitals. *J. Chem. Phys.* **2013**, *139*, Mikkelsen.
(64) Frisch, M. J.; Trucks, G. W.; Schlegel, H. B.; Scuseria, G. E.; Robb, M. A.; Cheeseman, J. R.; Scalmani, G.; Barone, V.; Mennucci, B.; Petersson, G. A.; et al. *Gaussian 09*, Revision B.01; Gaussian, Inc.: Wallingford, CT, 2010.
(65) Frisch, M. J.; Trucks, G. W.; Schlegel, H. B.; Scuseria, G. E.; Robb, M. A.; Cheeseman, J. R.; Scalmani, G.; Barone, V.; Mennucci, B.; Petersson, G. A.; et al. *Gaussian 09*, Revision D.01; Gaussian Inc.: Wallingford, CT, 2009.
(66) Grimme, S.; Antony, J.; Ehrlich, S.; Krieg, H. A Consistent and Accurate Ab Initio Parameterization of Density Functional Dispersion Correction (DFT-D) for the 94 Elements H-Pu. *J. Chem. Phys.* **2010**, *132*, 154104.
(67) Werner, H.-J.; Knowles, P. J.; Knizia, G.; Manby, F. R.; Schütz, M.; Celani, P.; Korona, T.; Lindh, R.; Mitrushenkov, A.; Rauhut, G.; et al.*MOLPRO*, version 2012.1, a package of ab initio programs, 2012. http://www.molpro.net.
(68) Neese, F. *WIREs Comput. Mol. Sci.* **2012**, *2*, 73−78.
(69) Henschel, H.; Navarro, J. C. A.; Yli-Juuti, T.; Kupiainen-Maatta, O.; Olenius, T.; Ortega, I. K.; Clegg, S. L.; Kurtén, T.; Riipinen, I.; Vehkamäki, H. Hydration of Atmospherically Relevant Molecular Clusters: Computational Chemistry and Classical Thermodynamics. *J. Phys. Chem. A* **2014**, *118*, 2599−2611.
(70) Temelso, B.; Archer, K. A.; Shields, G. C. Benchmark Structures and Binding Energies of Small Water Clusters with Anharmonicity Corrections. *J. Phys. Chem. A* **2011**, *115*, 12034−12046.

DOI: 10.1021/acs.jpca.5b09762
J. Phys. Chem. A 2016, 120, 621−630

(71) Jen, C. N.; McMurry, P. H.; Hanson, D. R. Stabilization of Sulfuric Acid Dimers by Ammonia, Methylamine, Dimethylamine, and Trimethylamine. *J. Geophys. Res.* **2014**, *119*, 7502−7514.
(72) Ortega, I. K.; Olenius, T.; Kupiainen-Määttä, O.; Loukonen, V.; Kurtén, T.; Vehkamäki, H. Electrical Charging Changes the Composition of Sulfuric Acid-Ammonia/Dimethylamine Clusters. *Atmos. Chem. Phys.* **2014**, *14*, 7995−8007.
(73) McGrath, M.; Olenius, T.; Ortega, I.; Loukonen, V.; Paasonen, P.; Kurtén, T.; Kulmala, M.; Vehkamäki, H. Atmospheric Cluster Dynamics Code: A Flexible Method for Solution of the Birth-Death Equations. *Atmos. Chem. Phys.* **2012**, *12*, 2345−2355.
(74) Olenius, T.; Schobesberger, S.; Kupiainen-Määttä, O.; Franchin, A.; Junninen, H.; Ortega, I. K.; Kurtén, T.; Loukonen, V.; Worsnop, D. R.; Kulmala, M.; et al. Comparing Simulated and Experimental Molecular Cluster Distributions. *Faraday Discuss.* **2013**, *165*, 75−89.
(75) Olenius, T.; Kurtén, T.; Kupiainen-Määttä, O.; Henschel, H.; Ortega, I. K.; Vehkamäki, H. Effect of Hydration and Base Contaminants on Sulfuric Acid Diffusion Measurement: A Computational Study. *Aerosol Sci. Technol.* **2014**, *48*, 593−603.

DOI: 10.1021/acs.jpca.5b09762
J. Phys. Chem. A 2016, 120, 621−630